Catalysis Today 175 (2011) 283–292

Contents lists available at ScienceDirect

Catalysis Today

journal homepage: www.elsevier.com/locate/cattod

Ultrasound enhanced catalytic ozonation of tetracycline in a rectangular air-lift reactor

Yan Wang, Hui Zhang*, Lu Chen

Department of Environmental Engineering, Wuhan University, P.O. Box C319, Luoyu Road 129#, Wuhan 430079, China

ARTICLE INFO

Article history:
Received 15 October 2010
Received in revised form 30 May 2011
Accepted 1 June 2011
Available online 13 July 2011

Keywords:
Catalytic ozonation
Ultrasonic irradiation
Goethite
Tetracycline
Rectangular air-lift reactor

ABSTRACT

The antibiotics tetracycline (TC) was degraded by ultrasound (US) enhanced catalytic ozonation using goethite catalyst (US/goethite/O_3) in a rectangular air-lift reactor. The effect of important operational parameters, including gaseous ozone concentration, gas flow rate, free radical scavenger, pH, and power density, on the removal of TC was investigated. The results showed that the TC removal followed pseudo-first-order kinetics and the removal rate increased with increasing gaseous ozone concentration, pH, gas flow rate and power density. The presence of free radical scavenger inhibited the removal rate to some extent. The catalyst stability was evaluated by measuring TC removal rate and iron leaching for three successive cycles. Almost no changes in the particle size and the surface area of the catalyst were observed before and after the reaction. The main intermediates were identified and the degradation pathway of TC was proposed. Toxicity test with *Daphnia magna* showed that the acute toxicity increased during the first stage of the reaction, and then gradually decreased with the progress of the oxidation.

1. Introduction

The ozonation process has been received increasing attention in treating pharmaceutical wastewaters due to its capability of oxidizing complex organic compounds into simpler and more easily biodegraded compounds [1,2]. However, its wide application was limited by low utilization and limit oxidizing power of ozone [3,4]. As a consequence, ozone was usually combined with other technology to enhance its oxidation power and to improve its utilization, including UV/O_3 [5,6], H_2O_2/O_3 [7,8], UV/H_2O_2/O_3 [9], US/O_3 [4,10] and catalytic ozonation [1,11–14].

Among the stated ozone-oxidation technologies, catalytic ozonation is considered as an effective technology to improve the degradation of the recalcitrant pollutants due to its capability of enhancing ozone decomposition [13–15]. Generally, catalytic ozonation includes homogeneous and heterogeneous catalytic ozonation. The heterogeneous catalytic ozonation has the low negative effect on water quality and the catalyst is easy to be separated from the reaction system [16,17]. However, catalyst deactivation in heterogeneous catalytic ozonation is a major problem due to the build-up of organic byproducts on the catalyst surface [18].

Recently, ultrasound has been used to combine with the heterogeneous advance oxidation processes (AOPs) [19,20]. When ultrasound is introduced into the reaction system, the transient cavitation can result in turbulent flow conditions within the reactor. This would accelerate overall mass transport of reactants and byproducts between the liquid phase and the catalyst surface [21,22]. In the meantime, the cavitational bubble collapse directly on the catalyst surface may cause direct damage by shock waves produced upon implosion, while cavitational collapse near the catalyst surface in the aqueous phase will cause microjets to hit the surface and produce a nonsymmetrical shock wave. This leads to continuous cleaning of the catalyst surface [22]. Therefore, ultrasound enhanced various heterogeneous AOPs including catalytic ozonation have been applied successfully in the degradation of a wide variety of pollutants [23,24].

As a well-known class of antibiotics, tetracycline hydrochloride (TC) was used globally to resist against infectious diseases for human and veterinary treatment [25]. Moreover, its large global consumption could result in the increasing presence of TC in the environment, which might threaten public health due to their propensity to select for resistant bacteria and facilitate the establishment and amplification of pathogenic reservoirs [26]. Especially in mainland China and Hong Kong, the enormous quantities of TCs were produced, imported, used and detected [26,27]. Therefore, TC was selected as a target refractory organic pollutant and was degraded by the combination of ultrasonic irradiation with catalytic ozonation in this study.

Compared with the conventional gas–liquid–solid reactors, the airlift reactor has the advantages of simple construction, feasible

* Corresponding author. Tel.: +86 27 68775837; fax: +86 27 68778893.
E-mail address: eeng@whu.edu.cn (H. Zhang).

0920-5861/$ – see front matter © 2011 Elsevier B.V. All rights reserved.
doi:10.1016/j.cattod.2011.06.001

Table 1
Chemical structure and relevant data for tetracycline hydrochloride.

Name	Tetracycline hydrochloride
Formula	$C_{22}H_{25}N_2O_8Cl$
structure	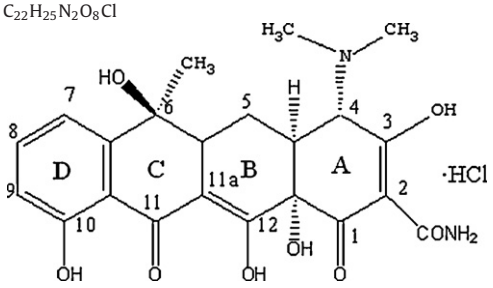
Formula weight (g mol^{-1})	480.5
Absorption (λ_{max}, nm)	359

scale-up, efficient mixing with low shear stress and energy consumption, as well as high gas–liquid mass transfer rate [9,28]. Particularly, the rectangular airlift reactor shows the better performance ratio than other kinds of airlift reactors [29,30]. In our previous study, a rectangular airlift reactor has been successfully employed for the decolorization of azo dye by ozonation in combination of ultrasonic irradiation [4]. Therefore, TC degradation was performed in a rectangular airlift reactor and the effect of operating conditions on TC removal by ultrasound enhanced catalytic ozonation using goethite catalyst (US/goethite/O_3) was investigated. The main intermediates were determined and the TC degradation pathway was proposed. The mineralization of TC and the toxicity test with *Daphnia magna* were also explored in this study.

2. Experimental

2.1. Materials

Goethite was obtained from Sigma–Aldrich and used as received. Tetracycline hydrochloride (AR Grade, 99%) was obtained from the market and used without further purification. The structure and relevant data for TC were shown in Table 1. Acetonitrile and methanol (HPLC Grade) were obtained from Shanghai Sinopharm Chemical Reagent Co. Ltd. (China). Both of oxalic acid and potassium iodide (AR grade) were obtained from Shanghai Zhangyun Chemical Co. Ltd. (China). Hydrogen peroxide (AR Grade, 30%, v/v) was obtained from Shanghai Yuanda Peroxide Co. Ltd. (China). tert-Butyl alcohol was obtained from Chengdu Institute of the Joint Chemical Reagent (China) and used as received.

2.2. Procedure

A stock solution of TC was prepared fresh in buffer solution composed of 0.05 mmol L^{-1} Na_2HPO_4 and KH_2PO_4 before each run and the initial concentration ($[TC]_0$) was set at 100 mg L^{-1}. The solution pH was measured with a Mettler Toledo FE20 pH-meter.

Semi-batch experiments were performed in a rectangular airlift reactor made of plexy glass (Fig. 1), which is similar to our previous study [4]. This reactor consists of a square column (50 mm × 50 mm) with the height of 120 mm, divided into a riser and a downcomer section by a plexy glass baffle (width: 50 mm; thickness: 4 mm; total height: 50 mm). The riser-to-downcomer cross-sectional area ratio is 1.3. The baffle was located at a distance of 12 mm from the bottom of the reactor. The gas distributor at the bottom of the riser was a perforated tube with six orifices of 1 mm diameter. Ozone was generated by electric discharge using 99.9% oxygen in a laboratory ozone generator (XFZ-5BI, China). Ozone concentrations in the gas and liquid phase were monitored by the iodometric method with potassium iodide solution and indigo method, respectively [31,32]. Then, a predetermined amount of goethite was added into the reactor containing 200 mL TC solution. A magnetic stirrer (Model 78-1, Hangzhou Instrument Motors Factory, China) provided complete mixing of the solution in the reactor.

Sonication was performed with a KS-250 ultrasonic generator (250 W, 20 kHz, Ninbo Kesheng Instrument Co., China) equipped with a titanium probe transducer. The tip of the probe was 1 cm in diameter and was placed 1.5 cm into the liquid layer. The sonication was administered in a pulse mode of 2.5 s on and 2.1 s off. The acoustic power (P) was determined calorimetrically [33]. At pre-selected time intervals, samples were taken by a syringe and filtered through 0.45 μm membranes before the TC concentration was measured.

2.3. Analysis methods

The TC concentration was measured using high-performance liquid chromatography (HPLC). HPLC is consisted of a LC-20AB pump, a Shimadzu HPLC system manager program and a SPD-10A UV-Vis detector. The maximum absorption wavelength was determined at 359 nm using a Shimadzu UV-1700 spectrophotometer to scan from 200 to 800 nm [34]. Aliquots of 20 μL were injected using an auto-sampler (SIL-20A Shimadzu). A shim-pack VP-ODS C18 (4.6 mm × 250 mm) packed with 5 μm spherical particles was used for separation. An acetonitrile/0.01 mol L^{-1} aqueous oxalic

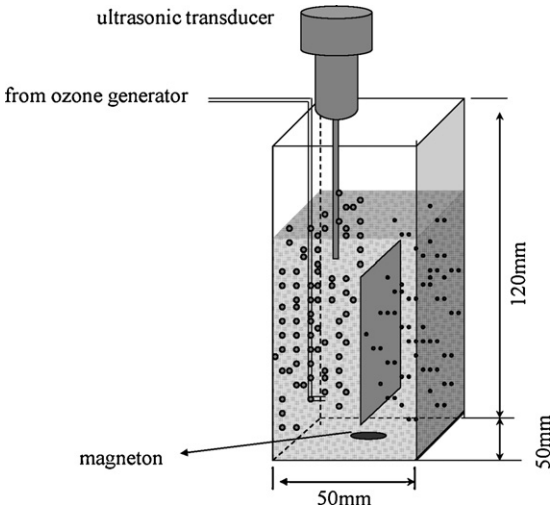

Fig. 1. Schematic view of the experimental setup.

acid (31:69, v/v) mixture of was used as mobile phase at room temperature with a constant flow rate of 1.0 mL min^{-1}.

Total organic carbon (TOC) was analyzed in a TOC analyzer (Multi N/C®2100, Analytik Jena AG) to evaluate the mineralization of TC. The acute toxicities were determined with *D. magna* immobilization essays. These tests were performed in accordance with testing conditions prescribed by OECD Guideline 202 [35]. *D. magna* was cultured in laboratory for more than three generations. The acute toxicity experiments were carried out in 50-mL-capacity test beakers using 25 24-h-old *D. magna*, which were divided to five groups. Four groups were performed as the test groups while one group as the blank one. They were set in the incubator along with testing samples. The incubator was set at 20 °C in a 16 h light-8 h dark cycle. No foods were given during the acute toxic test. Surviving and mobile *D. magna* was counted after 24 h.

In the case of the experiments on the catalyst stability and reusability, the catalyst was removed from the solution at the end of the experiments and washed gently with deionized water. Then, it was dried for 1 h in oven and the temperature was set at 100 °C. Iron leaching was evaluated by phenanthroline spectrophotometry [36]. The surface area of the catalyst was measured by nitrogen adsorption using an accelerated surface area (Micrometrics Gemini V2380, America). Particle size distribution of solid catalysts was measured in a MASTER-SIZER 3500 apparatus (Microtrac, America). This equipment determines the size distribution of particles dispersed in a liquid in the range 0.02–2800 μm using the Mie theory for measuring the light scattering behavior.

The intermediates during the reaction were detected by an Agilent 1100 instrument connected with an electrospray ionization (ESI) source operating in the positive ion mode. Depending on intermediates, gradient elution was used by varying the eluent ratio. The initial mobile phase composition was 5/95 (acetonitrile/0.01 mol L^{-1} aqueous oxalic acid), then this composition linearly changed to 35/65 in 10 min and the composition remained constant for 10 min, injection volume of 20 μL, and the UV detector set up at 359 nm. ESI source conditions were as follows: heated capillary temperature 200 °C; sheath gas (N_2) flow rate 20 units; spray voltage 4.5 kV; capillary voltage 25 V; tube lens offset voltage 25 V. The isolation width used in the MS^n experiments was 1 m/z unit. Total compounds mass spectra were scaned from 50 m/z to 800 m/z.

3. Results and discussion

3.1. Comparative performance for the different oxidation systems

To investigate the TC degradation in the different oxidation systems, experiments were performed with ozonation, catalytic ozonation, US/O_3 process, and US/goethite/O_3 process, respectively when the pH was fixed at 3, the gas flow rate was 30 L h^{-1} and the gas ozone concentration was 13.8 mg L^{-1}. Ultrasonic power was 85.7 W L^{-1} for the US/O_3 system and the US/goethite/O_3 system, while the addition of goethite was 0.5 g L^{-1} for the catalytic ozonation system and the US/goethite/O_3 system.

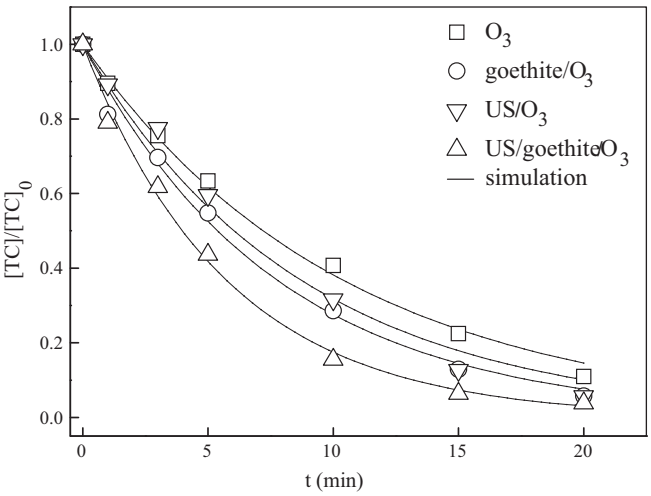

Fig. 2. Comparative performance for the different oxidation conditions on the TC removal ([TC] = 100 mg L^{-1}, $[O_3]_g$ = 13.8 mg L^{-1}, Q = 30 L h^{-1}, P = 85.7 W L^{-1}, [goethite] = 0.5 g L^{-1}, pH = 3).

As shown in Fig. 2, the removal of TC by all the above processes follows apparent pseudo-first-order kinetics according to the following rate equation:

$$-\frac{d[TC]}{dt} = k[TC] \quad (1)$$

where [TC] is the TC concentration at time t and k is the pseudo-first-order degradation rate constant. The k values were obtained and summarized in Table 2. The high R^2 values indicated that the apparent pseudo-first-order kinetics fitted the experimental data well.

Table 2 illustrates that only 0.096 min^{-1} rate constant was achieved by ozonation while the rate constant increased to 0.115 min^{-1} when ozonation was combined with ultrasonic irradiation. In the ultrasonic reactor, an energy gradient in the direction of propagation of the acoustic wave would be formed [37]. This corresponds to a force which would result in the turbulence when acting on a liquid and then would reduce the liquid film thickness of gas bubbles containing ozone [4,37]. Moreover, the break up of these gas bubbles due to ultrasonic irradiation would lead to the larger

Table 2
The pseudo-first-order rate constants under various operating conditions.

No.	$[TC]_0$ (mg L^{-1})	pH	Q (L h^{-1})	$[O_3]_g$ (mg L^{-1})	[Goethite] (g L^{-1})	P (W L^{-1})	k (min^{-1})	R^2
1	100	3	30	13.8	0	0	0.096 ± 0.003	0.996
2	100	3	30	13.8	0.5	0	0.129 ± 0.006	0.992
3	100	3	30	13.8	0	85.7	0.115 ± 0.007	0.988
4	100	3	30	13.8	0.5	85.7	0.174 ± 0.007	0.995
5	100	2	30	13.8	0.5	85.7	0.150 ± 0.007	0.993
6	100	5	30	13.8	0.5	85.7	0.244 ± 0.015	0.989
7	100	7	30	13.8	0.5	85.7	0.347 ± 0.030	0.983
8	100	9	30	13.8	0.5	85.7	0.401 ± 0.025	0.992
9	100	7	25	13.8	0.5	85.7	0.183 ± 0.004	0.998
10	100	7	40	13.8	0.5	85.7	0.500 ± 0.034	0.991
11	100	7	50	13.8	0.5	85.7	0.764 ± 0.045	0.995
12	100	7	30	23.5	0.5	51.2	0.370 ± 0.028	0.987
13	100	7	30	23.5	0.5	85.7	0.501 ± 0.022	0.996
14	100	7	30	23.5	0.5	101.9	0.580 ± 0.033	0.995
15	100	7	30	23.5	0.5	131.2	0.741 ± 0.033	0.997

specific surface area [38]. These effects can be considered as reasons for the enhancement of mass transfer of ozone from gaseous phase to aqueous phase [9,37–39]. In the meantime, the decomposition of ozone would produce thermolytically free radical with a high oxidizing power in the vapor phase of a cavitation bubble [3,9,40]:

$$O_3(g) +))) \rightarrow O_2(g) + O(^3P)(g) \quad (2)$$

$$O(^3P)(g) + H_2O \rightarrow 2^{\bullet}OH(g) \quad (3)$$

where the symbol "))))" indicates ultrasound. The generated free radicals may diffuse into the bulk solution to oxidize the TC. As a result, the removal rate in US/O_3 system would be higher than ozonation alone.

In parallel, catalytic ozonation could achieve 0.129 min^{-1} rate constant, which was also higher than 0.096 min^{-1} rate constant achieved by ozonation. It has been reported that the active sites of goethite could catalyze ozone decomposition and generate hydroxyl radicals [16,19]. As a result of its electrophilic character, ozone molecule could react with the Brönsted acid–OH_2^+ as well as neutral state of –OH to produce hydroxyl radicals via the following reactions [12,16]:

$$O_3 + \equiv Fe\text{-}OH_2^+ \rightarrow \equiv Fe\text{-}OH^{\bullet +} + {}^{\bullet}OH + O_2 \quad (4)$$

$$\equiv Fe\text{-}OH^{\bullet +} + H_2O \rightarrow \equiv Fe\text{-}OH_2^+ + {}^{\bullet}OH \quad (5)$$

$$O_3 + \equiv Fe\text{-}OH \rightarrow \equiv Fe\text{-}O^{\bullet -} + {}^{\bullet}OH + O_2 \quad (6)$$

$$O_3 + \equiv Fe\text{-}O^{\bullet -} \rightarrow \equiv Fe\text{-}OH + {}^{\bullet}OH + O_2 \quad (7)$$

Therefore, the generated hydroxyl radicals would attack TC at the surface of goethite or oxidize TC in the solution when they diffuse into the bulk liquid phase. This resulted in higher degradation rate achieved by catalytic ozonation than by ozonation alone. The separate adsorption experiment was performed when oxygen instead of the mixture of oxygen and ozone was bubbled into the reactor, and little TC removal was obtained (data not shown). This illustrated that the oxidation instead of adsorption was the dominant contribution to the TC removal.

When both ultrasonic irradiation and goethite catalyst were introduced into the ozonation system, TC removal rate reached 0.174 min^{-1}, which was nearly twice as high as that in ozonation alone and higher than that in catalytic ozonation or in US/O_3 system. As discussed above, TC oxidation by ozone would be improved when ultrasonic irradiation or catalyst was combined with ozonation. However, the active sites of the catalyst would be gradually occupied by the oxidation intermediates during catalytic ozonation process, which results in the catalyst deactivation [18]. In the presence of ultrasonic irradiation, the available active sites would be maintained due to the cleaning action of ultrasound [19,22]. In the meantime, ultrasound may cause the fragmentation of catalyst and increase the surface area as well as the active sites, and the turbulent effect of the cavitation could enhance mass transfer of the reactants and products to and from the catalyst [22]. On the other hand, the presence of solid catalyst may increase the formation of cavitations [23,41,42]. Therefore, compared to ozonation, catalytic ozonation and US/O_3, much higher degradation rate was achieved by US/goethite/O_3 system.

When oxygen instead of the mixture of oxygen and ozone was bubbled into the reactor, little TC removal was observed (data not shown). It illustrated the generated free radicals was negligible and consequently little TC could be degraded during the US/goethite process.

3.2. Effect of pH on the TC removal

The pH is usually considered as one of the most important parameters for ozonation in combination with ultrasound and catalyst. The investigated pH values were 2, 3, 5, 7, and 9, respectively, when initial TC concentration was 100 mg L^{-1}, the gas ozone concentration was 13.8 mg L^{-1}, the gas flow rate was 30 L h^{-1}, goethite addition was 0.5 g L^{-1} and ultrasonic power density was 85.7 W L^{-1}. As illustrated in Fig. 3, TC removal rate increased with the increasing pH, and the influence of pH on TC removal rate was significant before pH reached 7 while further increase in pH led to a slight increase in TC removal rate. It should be noted that there were four different species of the TC which could undergo protonation–deprotonation reactions depending on the pH of the aqueous solution [43]. When pH is less than 3, TC is fully protonated to be TCH^{3+}. With the increase of pH, the deprotonation degree of TC increases by three steps in succession via TCH_2, TCH^- and TC^{2-} [43]. Moreover, the deprotonated TC with a positively charged group would be more easily attacked by ozone molecules than TC itself while the pH does not reached 7 [44,45]. The degree of deprotonation is enhanced with the increase of the pH, which results in the increasing removal rate accordingly. However, the fraction of TCH^- and TC^{2-} is predominant while pH exceeds 7 and their effect on the TC removal rate may not be greater than that of TCH^{3+} or TCH^2 when pH < 7. Thus, the removal rate of TC increased from 0.150 to 0.347 min^{-1} when pH values increased from 2 to 7, while it increased to only 0.401 min^{-1} when pH reached 9.

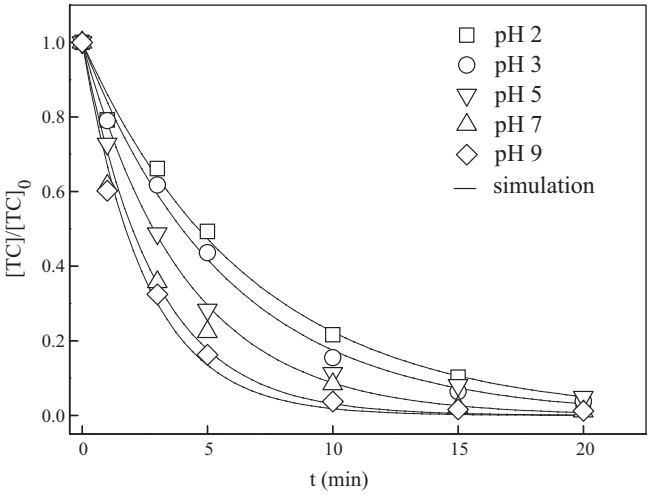

Fig. 3. The effect of pH on the TC removal ([TC] = 100 mg L^{-1}, $[O_3]_g$ = 13.8 mg L^{-1}, Q = 30 L h^{-1}, P = 85.7 W L^{-1}, [goethite] = 0.5 g L^{-1}).

On the other hand, the decomposition rate of ozone also depended on the pH. Because the different reactivity of ozone is related to the three different types of the goethite surface functional groups ($\equiv FeOH_2^+$, $\equiv FeOH$, $\equiv FeO^-$) which are influenced by the solution pH [12]. The surface functional groups of goethite changed with the pH as the following equations [12,20,46]:

$$\equiv FeOH_2^+ \leftrightharpoons \equiv FeOH + H^+, \qquad pK_a = 6.4 \quad (8)$$

$$\equiv FeOH \leftrightharpoons \equiv FeO^- + H^+, \qquad pK_a = 9.2 \quad (9)$$

Due to its nucleophilic and electrophilic character [16,47], ozone molecule may react with the surface hydroxyl groups of goethite, such as $\equiv FeOH_2^+$, $\equiv FeOH$ and $\equiv FeO^-$, to generate hydroxyl radicals [16,46]. Moreover, the catalytic activity of goethite reached the maximum when the pH was 7, because the relatively weak FeO–H bonds of goethite represented a high affinity for molecular ozone and was easy for the surface OH–ozone combination [46]. Thus, the removal rate of TC increased with the increasing pH when the pH < 7 and the increase became insignificant when the pH > 7.

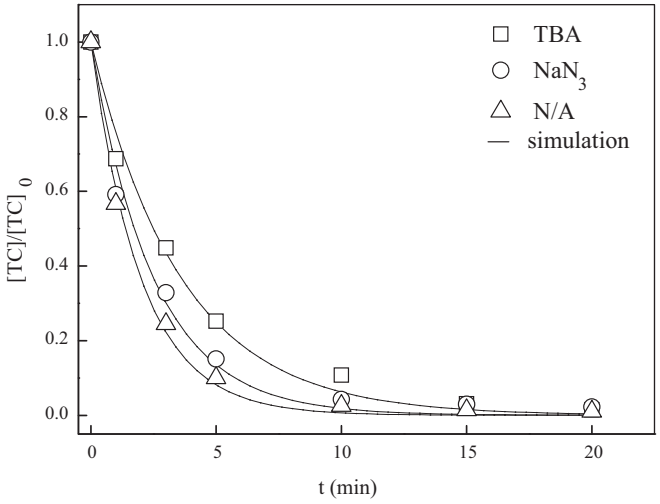

Fig. 4. The effect of free-radical scavenger on the TC removal ([TC] = 100 mg L^{-1}, $[O_3]_g$ = 23.5 mg L^{-1}, Q = 30 L h^{-1}, P = 85.7 W L^{-1}, [goethite] = 0.5 g L^{-1}, pH = 7).

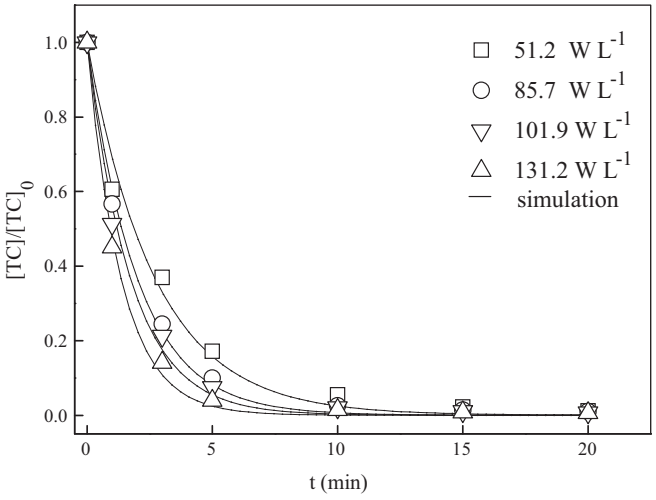

Fig. 5. The effect of power density on the TC removal ([TC] = 100 mg L^{-1}, $[O_3]_g$ = 23.5 mg L^{-1}, Q = 30 L h^{-1}, [goethite] = 0.5 g L^{-1}, pH = 7).

3.3. Effect of free-radical scavenger on the TC removal

To further determine whether the free radical reaction played an major role on the degradation rate of TC in the US/goethite/O_3 system, some free radical scavengers were employed when the TC concentration was 100 mg L^{-1}, gaseous ozone concentration was 23.5 mg L^{-1}, ultrasonic power density was 85.7 W L^{-1}, goethite addition was 0.5 g L^{-1}, the gas flow rate was 30 L h^{-1} and the pH was 7. The hydroxyl radical and singlet oxygen are considered to be the main oxide species during the ozonation process [48]. Then the addition of tert-butyl alcohol (TBA) as a stronger hydroxyl radical scavenger [13], or sodium azide as a singlet oxygen scavenger [49] was investigated in the US/goethite/O_3 system. It could be seen from Fig. 4 that the removal rate of TC were 0.277 and 0.408 min^{-1}, respectively when 0.015 mol L^{-1} TBA and 0.078 mol L^{-1} sodium azide were applied to the reaction system. The degradation rates are relatively lower compared with 0.501 min^{-1} degradation rate of TC in the absence of any free radical scavenger. This indicates that free radicals generated in the US/goethite/O_3 system improve the TC degradation, but the direct ozone reaction still plays the major role in this system.

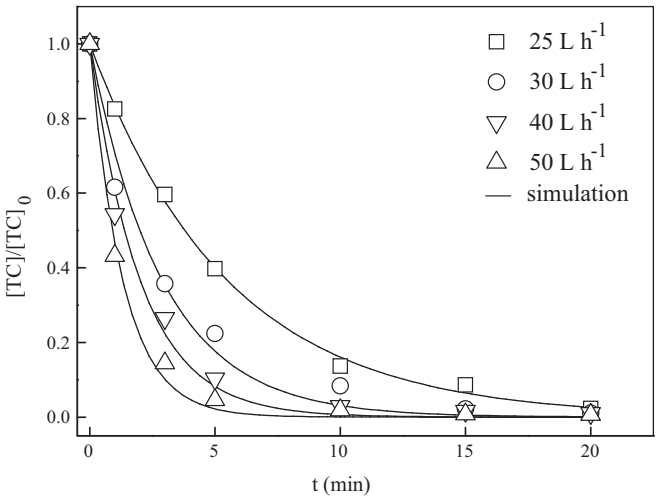

Fig. 6. The effect of gas flow rate on the TC removal ([TC] = 100 mg L^{-1}, $[O_3]_g$ = 13.8 mg L^{-1}, P = 85.7 W L^{-1}, [goethite] = 0.5 g L^{-1}, pH = 7).

3.4. Effect of power density on the TC removal

The degradation of TC by ultrasound enhanced catalytic ozonation with goethite at different power densities was studied when the initial TC concentration was 100 mg L^{-1}, gas ozone concentration was 23.5 mg L^{-1}, the gas flow rate was 30 L h^{-1} and pH was 7. As observed in Fig. 5, the degradation rate of TC increased from 0.370 to 0.741 min^{-1} when the power densities increased from 51.2 W L^{-1} to 131.2 W L^{-1}. It was reported that ultrasound could cause the fragmentation of catalyst and consequently increase the surface area as well as the active sites of the catalyst [49]. To confirm this point, the surface area of goethite before and after ultrasonic irradiation under various power densities was determined and the result was shown in Table 3. As can be seen in Table 3, negligible change of the surface area of goethite was observed after ultrasonic irradiation, which was similar to the results by Muruganandham et al. when the azo dye Direct Orange 39 was decolorized by US/goethite/H_2O_2 process [50]. Table 3 also indicated that the increase of power density led to the little variation in the surface area of goethite.

With the increase in the power density, the cavitation effect would be accelerated [51]. This results in the enhancement of ozone mass transfer from gas phase to liquid phase and mass transport of the reactants and products between the liquid phase and the catalyst surface [22,51,52]. In addition, the cleaning action of ultrasound and the generation of free radial from ozone decomposition would also be improved with the increase of cavitation effect. These effect rather than the increase of surface area can be considered as reasons for the fact that TC removal rates increase with power density.

Table 3
The surface area of goethite before and after ultrasonic irradiation.

Parameters	Fresh	Used (51.2 W L^{-1})	Used (85.7 W L^{-1})	Used (101.9 W L^{-1})	Used (131.2 W L^{-1})
BET surface area (m^2 g^{-1})	10.669	10.625	10.658	10.677	10.643
Langmuir surface area (m^2 g^{-1})	16.867	16.888	16.938	16.991	16.900
Single-point surface area (p/p_0) (m^2 g^{-1})	10.430	10.329	10.382	10.376	10.352

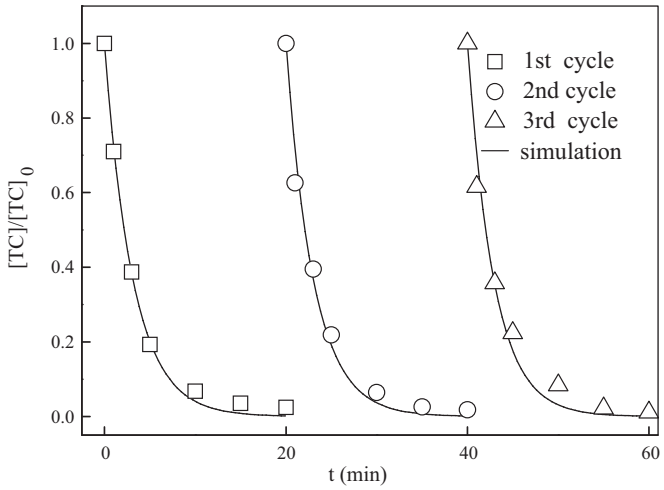

Fig. 7. Recycling study of the degradation of TC ([TC] = 100 mg L^{-1}, $[O_3]_g$ = 13.5 mg L^{-1}, Q = 30 L h^{-1}, P = 85.7 W L^{-1}, [goethite] = 0.5 g L^{-1}, pH = 7).

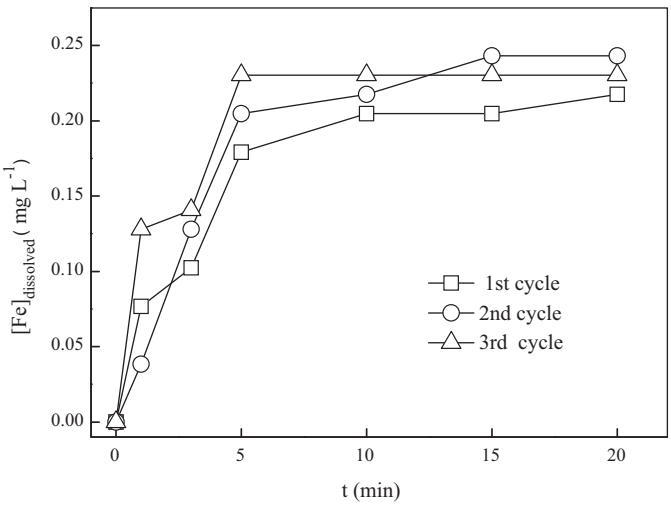

Fig. 9. The iron leaching during three cycles of reaction.

3.5. Effect of gas flow rate on the TC removal

The removal rate of TC in the US/goethite/O_3 system was investigated at different gas flow rate when the TC concentration was 100 mg L^{-1}, gaseous ozone concentration was 13.8 mg L^{-1}, ultrasonic power density was 85.7 W L^{-1}, goethite addition was 0.5 g L^{-1} and the pH was 7. It can be seen in Fig. 6 that the degradation rate increases with the increase of the gas flow rate. The apparent degradation rate constants were 0.183, 0.347, 0.500 and 0.764 min^{-1} when gas flow rates were 25, 30, 40 and 50 L h^{-1}, respectively. The increase in the flow rate corresponds to a larger net surface area for mass transfer of ozone from the gas phase to the aqueous phase, which results in the increase of the volumetric mass transfer coefficient of ozone [53] and consequently the increase of mass transfer rate of ozone from gas phase to liquid phase. Then more ozone would be available to oxidize TC.

3.6. Stability of the catalyst in ultrasound enhanced catalytic ozonation reaction

To evaluate the stability and reusability of the goethite catalyst in the US/goethite/O_3 system, the experiment was carried out when the TC concentration was 100 mg L^{-1}, gaseous ozone concentration was 13.5 mg L^{-1}, ultrasonic power density was 85.7 W L^{-1}, goethite addition was 0.5 g L^{-1}, the gas flow rate was 30 L h^{-1}, and the pH was 7. As shown in Fig. 7, the removal rates of TC were nearly unchanged for three successive cycles, which were 0.320, 0.331, 0.347 min^{-1}, respectively. It confirmed that goethite had the long-term reusability and activity in the US/goethite/O_3 system.

The particle size distribution of the fresh and used goethite after three runs under the same condition was evaluated and depicted in Fig. 8. The results show that the particle size distribution is located between 0.2 μm and 300 μm with a maximum at 15 μm before and after reaction. In this study, almost no changes were detected for the catalyst particle size after ultrasonic irradiation. The similar phenomenon was reported by Kim et al. when ultrasound in combination with heterogeneous Fenton-like system was used to degrade *p*-chlorophenolin [41]. Thus, the particle size distribution before and after ultrasonic irradiation illustrates that goethite keeps stable structure in the US/goethite/O_3 system.

The amount of iron dissolved in the solution was determined during the three consecutive US/goethite/O_3 experiments as shown in Fig. 9. The maximum concentration of the iron in solution is less than 0.25 mg L^{-1}, which can be neglected compared with the

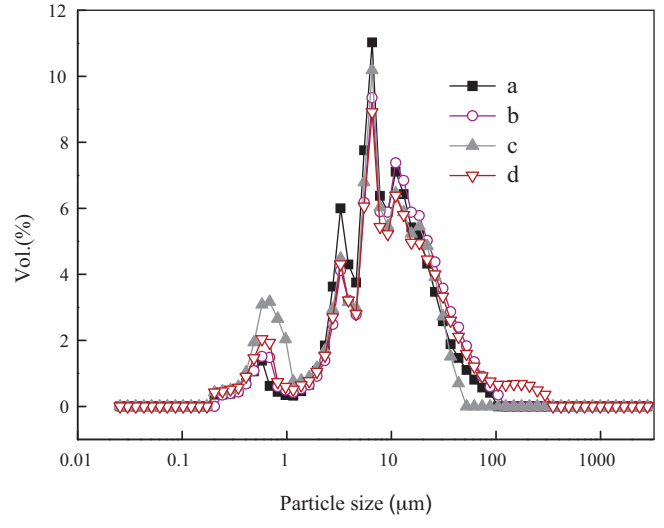

Fig. 8. Goethite catalyst particles size distribution dispersed in water before reaction (a), after the first cycle (b), after two cycles (c) and after three cycles of reaction (d).

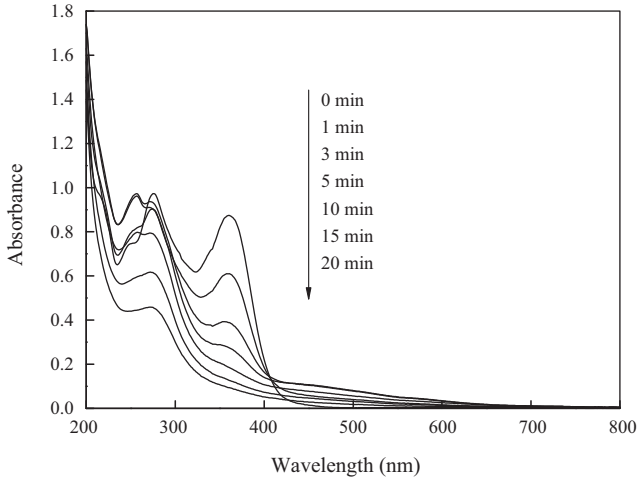

Fig. 10. UV–Vis spectral changes with reaction time ([TC] = 100 mg L^{-1}, $[O_3]_g$ = 23.5 mg L^{-1}, Q = 30 L h^{-1}, P = 85.7 W L^{-1}, [goethite] = 0.5 g L^{-1}).

Table 4
Main fragment ions obtained from MS and MS/MS analyses of tetracycline and transformation products.

Compounds	Observed fragments ions at *m*/*z* vale	
	MS	MS/MS
Tetracycline	445	427, 410
Product 1	461	444, 400 443, 426
Product 2	477	461, 442
Product 3	443	426, 408
Product 4	509	448, 430
Product 5	491	474, 430
Product 6	447	430, 412
Product 7	383	366, 347

standard effluent discharge and further confirms the stability and reusability of goethite in the US/goethite/O_3 system.

3.7. The degradation mechanism of TC in the US/goethite/O_3 system

The degradation of TC in aqueous solution by ultrasound enhanced catalytic ozonation with goethite was initially monitored by UV–Vis spectroscopy to clarify the changes of molecular and structural characteristics of TC. The UV–Vis spectra of the initial solution of TC and the aliquots withdrawn after successive reaction times were plotted from 200 nm to 800 nm in Fig. 10. As could be observed from these spectra, before the oxidation, the absorbance of TC in water was characterized by two main wavelengths. One band was located at the visible region, with its maximum absorption at 359 nm when another band in the ultraviolet region located

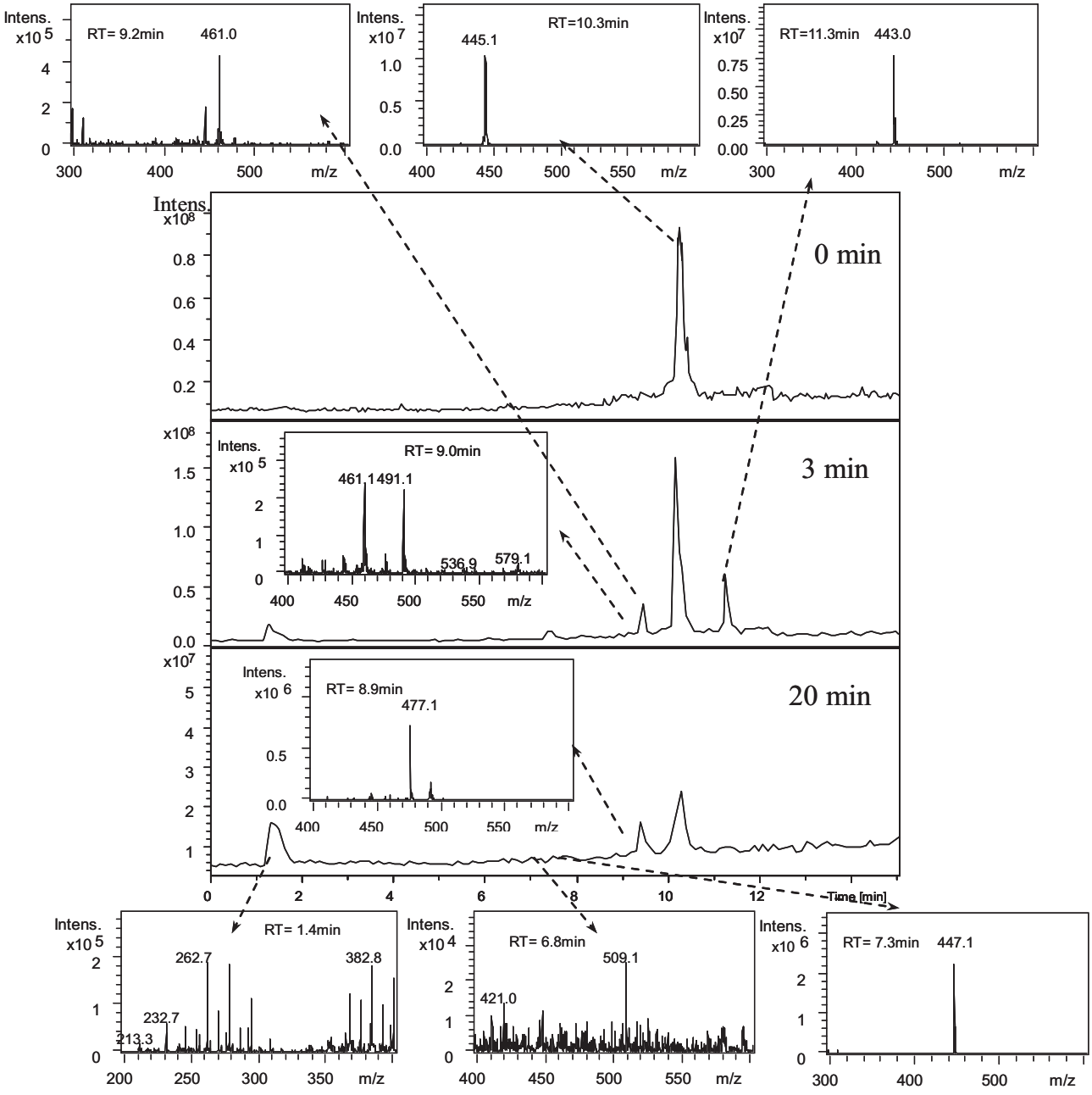

Fig. 11. LC–ESI(+)-MS total ion chromatograms for monitoring of the degradation of tetracycline by O_3 in aqueous medium after reaction times of 0, 3 and 20 min. The insets show the mass spectra of the products eluted at 1.4, 6.8, 7.3, 8.9, 9, 9.2, 10.3 and 11.3 min.

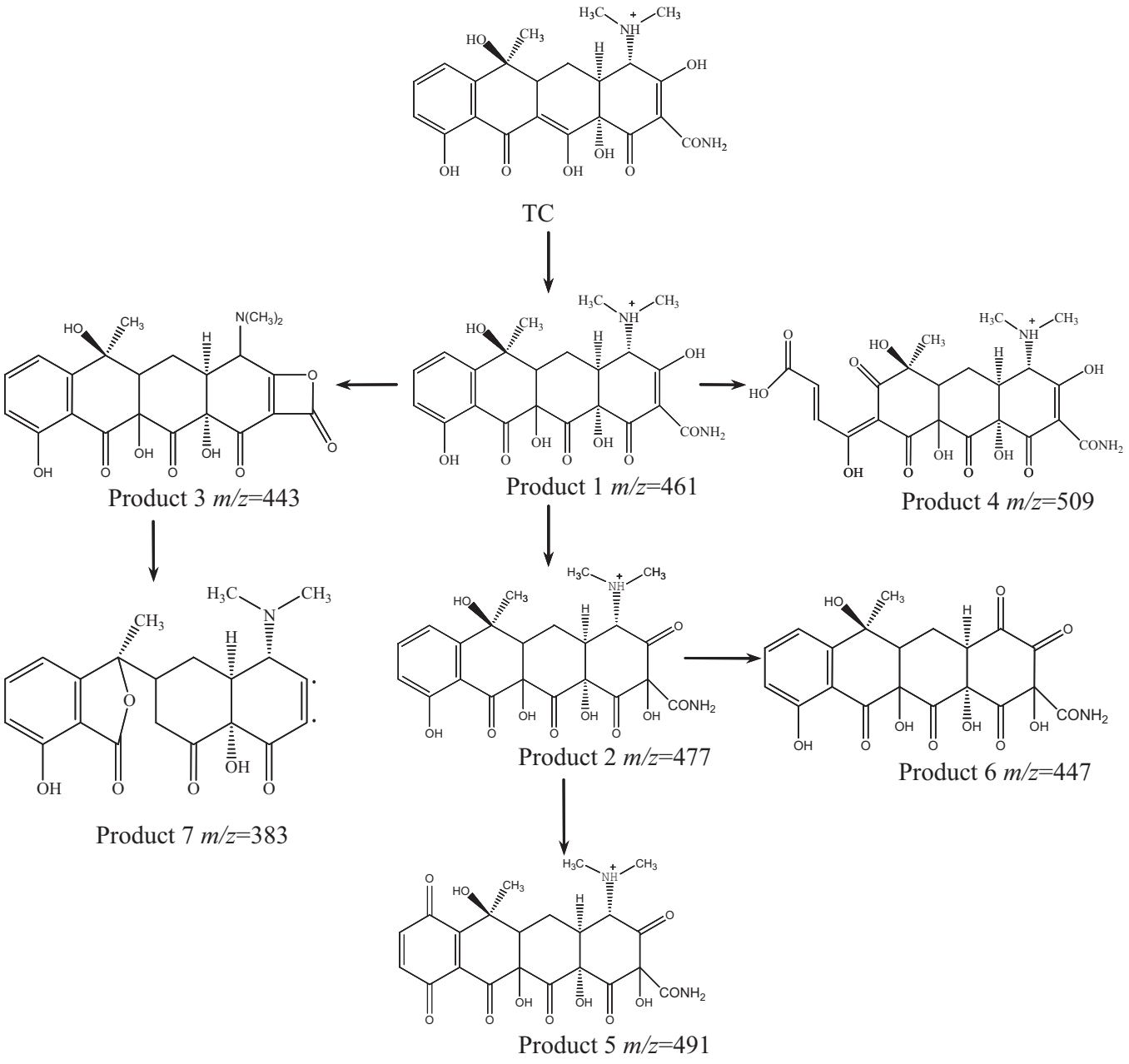

Fig. 12. Proposed degradation pathway of TC.

at 275 nm. The peak at 275 nm was associated with aromatic ring A structure including acylamino and hydroxyl in the molecule (Table 1), and that at 359 nm was originated from aromatic rings B–D (Table 1), comprising the extended chromophores [54]. The disappearance of two bands continuously decreased with the reaction time, which was due to the fragmentation of enolic groups connected to aromatic ring B and acylamino and enolic groups connected to the aromatic ring A by oxidation spices attack. Moreover, byproducts with the similar chemical structures to that of TC were continuously formed when TC was consumed simultaneously.

The oxidation of TC is involved in a series of reactions leading to the formation of intermediate products. Thus, simple methods for the direct detection of reactive intermediates were important for explaining and understanding the degradation pathway of TC. From the HPLC–UV chromatograms obtained from aliquots collected at different reaction times (data not shown), it demonstrated that the intensity of TC decreased while the reaction proceeded. At the same time the new peaks were detected and they increased as TC decreased. Moreover, their retention times were shorter than that of TC, which illustrated that more polar intermediate compounds were formed during the oxidation of TC.

To further identify the intermediate products during the oxidation, an electrospray ionization (ESI) source method was employed. The total ion chromatograms of the degraded TC by the ultrasound enhanced catalytic ozonation with goethite at 0, 3 and 20 min were represented Fig. 11. The peak of TC and the peaks of seven major byproducts were observed. The overall MS and MS/MS characteristics corresponding to the peaks were gathered in Table 4.

As shown in Fig. 11, an intense and prominent ion of m/z 445 was observed in the MS spectrum and its retention time was 10.3 min, corresponding to the deprotonated molecular ion. The successive mass-selection of the main precursor ions was proposed and their fragmentation upon collision-induced dissociation was yielded by the following sequence: m/z 445 → m/z 427(by loss of H_2O) → m/z

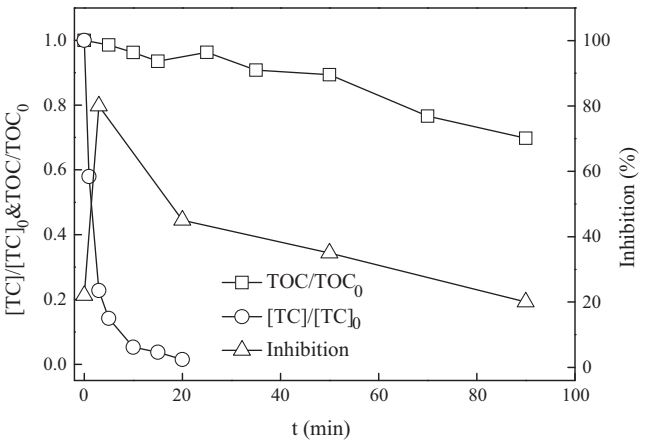

Fig. 13. Decay of TC and variation of toxicity in US/goethite/O_3.

410 (then by loss of NH_3) (ESI(+)-MS^2). Based on the description in literature [25], the fragmentation pathway of the water loss was proposed to be the oxidation of the hydroxyl group bound at the C6 atom. Besides TC, seven immediate products of m/z 461, 383, 443, 447, 477, 491 and 509, were also detected. Based on the results and the literature, the possible TC degradation pathway was proposed as illustrated in Fig. 12. The TC structure indicated that the C11a–C12 double bond is only one electron-withdrawing substituent and is much more susceptible to the ozone or free radical attack than the other available double bonds, such as C2–C3 double bond and ring D. Then the initial 1,3-dipolar cycloaddition towards the C11a–C12 double bond of TC gave rise to the formation of Product 1. The C2–C3 double bond of Product 1 was further attacked by ozone or hydroxyl radical to form Products 2 and 3, respectively, while the attack of ring D of Product 1 led to the destruction of the aromatic ring and the generation of Product 4 [43]. Product 3 was further oxidized to Product 7 with an m/z value of 383. The attack of dimethyl amino group and ring D of Product 2 resulted in the formation of Products 5 and 6 of m/z 491 and 447 [47,56].

3.8. Mineralization and acute toxicity tests of TC

To investigate the mineralization of TC in the US/goethite/O_3 system, experiments were performed when the TC concentration was 100 mg L^{-1}, pH was 7, the gas flow rate was 30 L h^{-1}, gaseous ozone concentration was 13.8 mg L^{-1}, ultrasonic power density was 85.7 W L^{-1}, and goethite addition was 0.5 g L^{-1}. As shown in Fig. 13, less than 4% TOC was removed after 20 min reaction compared with 99.2% TC removal efficiency. After the reaction time was extended to 90 min, 30% of TOC removal efficiency could be achieved and further prolong of reaction time may increase TOC removal.

The variation of acute toxicity during US/goethite/O_3 process was evaluated by 24-h immobilization test with *D. magna*. As can be seen in Fig. 13, the initial solution of TC leads to 20% death of the crustacean. The acute toxicity increased significantly after 3 min reaction, and 80% death of *D. magna* was observed. This is due to the generation of more toxic immediate products [57,58], and the similar tendency was reported by Beltrán et al. [58] and Wu et al. [59]. With the further progress of reaction, the acute toxicity reduced gradually, indicating the toxic structures were destructed and the immediate products were degraded into the less toxic products.

4. Conclusion

Tetracycline could be readily decomposed by the catalytic ozonation combined with ultrasonic irradiation. TC removal rate increased with the increase of power density and pH. The presence of the free radical scavenger (sodium azide or tert-butyl alcohol) inhibited TC removal rate, indicating both direct molecular ozone reaction and indirect radical reaction were involved in the US/goethite/O_3 system. TC was oxidized quickly by ozone, free radical, or both via 1,3-dipolar cycloaddition and electrophilic reactions to form immediate products. After three successive cycles, TC removal rate and the particle size distribution of goethite change insignificantly, and the dissolved iron concentration was very low, indicating the stability of catalyst in US/goethite/O_3 system. The toxicity assessed by *D. magna* decreased after it reached the maximum during the first period of the oxidation.

Acknowledgements

This study was supported by Natural Science Foundation of China (Grant No. 20977069), Natural Science Foundation of Hubei Province, China through "The Outstanding Youth Scholars Program" (Grant No. 2007ABB028) and Wuhan Municipal Science and Technology Bureau, China through "The Chenguang Project" (Grant No. 20015005061). We appreciate the anonymous reviewers for their valuable comments and suggestions.

References

[1] F.J. Beltrán, P. Pocostales, P.M. Álvarez, F. López-Piñeiro, Appl. Catal. B: Environ. 92 (2009) 262.
[2] B. Ning, N.J.D. Graham, J. Environ. Eng. 134 (2008) 994.
[3] H. Zhang, L.J. Duan, D.B. Zhang, J. Hazard. Mater. B 138 (2006) 53.
[4] H. Zhang, Y.J. Lv, F. Liu, D.B. Zhang, Chem. Eng. J. 138 (2008) 231.
[5] J.L. Graham, R. Striebich, C.L. Patterson, E.R. Krishnan, R.C. Haught, Chemosphere 54 (2004) 1011.
[6] Y.F. Rao, W. Chu, J. Hazard. Mater. 180 (2010) 514.
[7] I.A. Balcioğlu, M. Otker, Chemosphere 50 (2003) 85.
[8] A.Y.C. Lin, C.F. Lin, J.M. Chiou, J. Hazard. Mater. 171 (2009) 452.
[9] R. Andreozzi, V. Caprio, R. Marotta, D. Vogna, Water Res. 37 (2003) 993.
[10] V. Naddeo, V. Belgiorno, D. Ricco, D. Kassinos, Ultrason. Sonochem. 16 (2009) 790.
[11] L. Yang, C. Hu, Y.L. Nie, J.H. Qu, Environ. Sci. Technol. 43 (2009) 2525.
[12] J.S. Park, H. Choi, J. Cho, Water Res. 38 (2004) 2285.
[13] B. Kasprzyk-Hordern, M. Ziółek, J. Nawrocki, Appl. Catal. B: Environ. 46 (2003) 639.
[14] M.H. Khan, J.Y. Jung, Chemosphere 72 (2008) 690.
[15] B. Legube, N.K.V. Leitner, Catal. Today 53 (1999) 61.
[16] M.H. Sui, L. Sheng, K.X. Lu, F. Tian, Appl. Catal. B: Environ. 96 (2010) 94.
[17] Z.Q. He, R.Y. Zhu, X. Xu, S. Song, J.M. Chen, Ind. Eng. Chem. Res. 48 (2009) 5578.
[18] H. Einaga, S. Futamura, J. Catal. 243 (2006) 446.
[19] M. Muruganandham, J.J. Wu, Catal. Commun. 8 (2007) 668.
[20] H. Zhang, H. Fu, D.B. Zhang, J. Hazard. Mater. 172 (2009) 654.
[21] H. Zhang, L.J. Duan, Y. Zhang, F. Wu, Dyes Pigments 65 (2005) 39.
[22] B. Neppolian, J.S. Park, H. Choi, Ultrason. Sonochem. 11 (2004) 273.
[23] H. Liu, M.Y. Liang, C.S. Liu, Y.X. Gao, J.M. Zhou, Chem. Eng. J. 153 (2009) 131.
[24] R. Chand, N.H. Ince, P.R. Gogate, D.H. Bremner, Sep. Purif. Technol. 67 (2009) 103.
[25] I. Dalmázio, M.O. Almeida, R. Augusti, J. Am. Soc. Mass. Spectrom. 18 (2007) 679.
[26] Y. Luo, L. Xu, M. Rysz, Y.Q. Wang, H. Zhang, P.J.J. Alvarez, Environ. Sci. Technol. 45 (2011) 1827.
[27] B.J. Richardson, P.K.S. Lam, M. Martin, Mar. Pollut. Bull. 50 (2005) 913.
[28] W. Yu, T.F. Wang, M.L. Liu, F.F. Song, Ind. Eng. Chem. Res. 49 (2010) 11752.
[29] A. Couvert, M. Roustan, P. Chatellier, Chem. Eng. Sci. 54 (1999) 5245.
[30] B. Gourich, N. EL Azher, M.S. Bellhaj, H. Delmas, A. Bouzidi, M. Ziyad, Chem. Eng. Process. 44 (2005) 1047.
[31] D.L. Flamm, Environ. Sci. Technol. 11 (1977) 978.
[32] H. Bader, J. Hoingé, Water Res. 154 (1981) 449.
[33] T. Kimura, T. Sakamoto, J.M. Leveque, H. Sohmiya, M. Fujita, S. Ikeda, T. Ando, Ultrason. Sonochem. 3 (1996) S157.
[34] H. Zhang, F. Liu, X.G. Wu, J.H. Zhang, D.B. Zhang, Asia Pac. J. Chem. Eng. 4 (2009) 568.
[35] Organization for Economic Cooperation and Development (OECD), Daphnia sp. Acute Immobilization Test, Test Guideline No. 202, OECD Guidelines for Testing of Chemicals, 2004.
[36] Z.O. Tesfaldet, J.F.V. Staden, R.I. Stefan, Talanta 64 (2004) 1189.
[37] L.K. Weavers, M.R. Hoffmann, Environ. Sci. Technol. 32 (1998) 3941.
[38] R. Lall, R. Mutharasan, Y.T. Shah, P. Dhurjati, Water Environ. Res. 75 (2003) 171.
[39] E. Dahi, Water Res. 10 (1976) 677.
[40] W. Yue, P.J. Yao, Y.N. Wei, H.T. Mo, Polym. Degrad. Stabil. 93 (2008) 1814.
[41] J.K. Kim, F. Martinez, I.S. Metcalfe, Catal. Today 124 (2007) 224.
[42] D. Drijvers, H. Van Langenhove, M. Beckers, Water Res. 33 (1999) 1187.
[43] M.E. Parolo, M.C. Savini, J.M. Vallés, Appl. Clay Sci. 40 (2008) 179.

[44] M.H. Khan, H. Bae, J.Y. Jung, J. Hazard. Mater. 181 (2010) 659.
[45] F.J. Beltrán, J.M. Encinar, J.F. González, Water Res. 31 (1997) 2415.
[46] T. Zhang, C.J. Li, J. Ma, H. Tian, Z.M. Qiang, Appl. Catal. B: Environ. 82 (2008) 131.
[47] F.J. Beltrán, Ozone Reaction Kinetics for Water and Wastewater Systems, Lewis Publisher, 2004.
[48] E. Naffrechoux, S. Chanoux, C. Petrier, J. Suptil, Ultrason. Sonochem. 7 (2000) 255.
[49] Y. Lion, M. Delmelle, A.V. DE Vorst, Nature 263 (1976) 442.
[50] M. Muruganandham, J.S. Yang, J.J. Wu, Ind. Eng. Chem. Res. 46 (2007) 691.
[51] Y.N. Liu, D. Jin, X.P. Lu, P.F. Han, Ultrason. Sonochem. 15 (2008) 755.
[52] J.G. Wang, X.K. Wang, G.L. Li, P.Q. Guo, Z.X. Luo, J. Hazard. Mater. 176 (2010) 333.
[53] J.W. Kang, M.J. Hoffmann, Environ. Sci. Technol. 32 (1998) 3194.
[54] W. Diirckheimer, Angew. Chem. 14 (1975) 721.
[56] M.C. Dodd, M. Buffle, U.V. Gunten, Environ. Sci. Technol. 40 (2006) 1969.
[57] F.J. Beltrán, P. Pocostales, P. Alvarez, A. Oropesa, J. Hazard. Mater. 163 (2009) 768.
[58] F.J. Beltrán, A. Aguinaco, J.F. García-Araya, A. Oropesa, Water Res. 24 (2008) 3799.
[59] G. Wu, Y.X. Jiang, L.Y. Zha, Z.M. Ye, Z.F. Zhou, J.F. Ye, H.W. Zhou, Can. J. Civil Eng. 37 (2010) 1485.